ФИЗИКА ЭЛЕМЕНТАРНЫХ ЧАСТИЦ И АТОМНОГО ЯДРА
2016. Т. 47. ВЫП. 6

REACTOR TARGET FROM METAL CHROMIUM FOR "PURE" HIGH-INTENSIVE ARTIFICIAL NEUTRINO SOURCE

V. N. Gavrin[1], *Yu. P. Kozlova*[1,*], *E. P. Veretenkin*[1], *A. V. Logachev*[2], *A. I. Logacheva*[2], *I. S. Lednev*[3], *A. A. Okunkova*[3]

[1] Institute for Nuclear Research of the Russian Academy of Sciences, Moscow

[2] JSC "Kompozit", Korolev, Russia

[3] Moscow State University of Technology "STANKIN", Moscow

The paper presents the first results of development of manufacturing technology of metallic chromium targets from highly enriched isotope ^{50}Cr for irradiation in a high flux nuclear reactor to obtain a compact high-intensity neutrino source with low content of radionuclide impurities and minimum losses of enriched isotope. The main technological stages are the hydrolysis of chromyl fluoride, the electrochemical reduction of metallic chromium, the hot isostatic pressing of chromium powder and the electrical discharge machining of chromium bars. The technological stages of hot isostatic pressing of chromium powder and of electrical discharge machining of Cr rods have been tested.

PACS: 95.55.Vj

INTRODUCTION

The artificial neutrino sources with intensity at the level of 0.5–1.5 MCi based on radionuclide ^{51}Cr were used in the calibration experiments SAGE and GALLEX [1, 2]. The weighted-average result of these experiments, expressed as the ratio R of the measured neutrino capture rate to the expected rate based on the measured source intensity and the known neutrino capture cross section, calculated by J. Bahcall [3], gives $R = 0.87 \pm 0.05$, considerably less than the expected value of unity.

A possible explanation for such a low result could be overestimation of the cross section for neutrino capture to the two lowest excited levels in ^{71}Ge. However, the highly precise measurements of the contribution of the excited levels performed at the RCNP (Osaka, Japan) [4] did not confirm this hypothesis.

*E-mail: julia@inr.ru

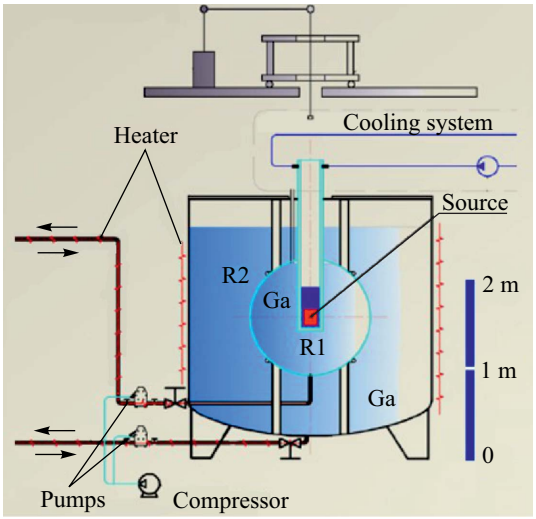

Fig. 1. The schematic drawing of the proposed experiment BEST

The other reason could be statistical fluctuation, but its probability is rather small, about 5%. At last, the reason could be real physical effect, a possible transition of active neutrino into sterile states at very short baselines with large Δm^2 [5].

The interpretation of Ga source experiments in terms of oscillations to sterile neutrino with $\Delta m^2 \sim 1$ eV^2 is also in good agreement with anomalous results of the experiments LSND [6] and MiniBooNE [7] as well as with results of some refinement of cosmological and reactor data [8]. Given the potential implication of sterile neutrino, it is important to confirm their existence in multiple approaches [5]. In the article, we consider the possibility of production of metal chromium target for a $>\sim 3$ MCi ^{51}Cr neutrino source to be applied in the experiment BEST [9] to search for sterile transitions at the Baksan Neutrino Observatory, INR RAS.

The schematic drawing of the proposed short baseline experiment is given in Fig. 1. An artificial ^{51}Cr neutrino source with initial activity of ~ 3 MCi will be placed in the center of a 50-t target of liquid Ga metal that is divided into two concentric spherical zones, an inner 7.5-t zone and an outer 42.5-t zone, that provide the same pass length of 55 cm in each zone.

The probability that neutrino with energy E survives after passing the distance L from the source (survival probability) is described by the expression:

$$P_{ee} = 1 - \sin^2 2\theta \sin^2(1.27\Delta m^2 L/E),$$

where Δm^2 is squared mass difference of neutrino eigenstates and θ is mixing angle.

The statistically significant differences between the values of neutrino capture rate in the zones can give a direct proof of a real physical effect, the possible transitions of active neutrinos into sterile states.

One of the main stages in realizing of the project BEST is production of a compact high-intensive artificial neutrino source based on ^{51}Cr with high radionuclide purity.

1. ^{51}Cr TARGET MANUFACTURING

1.1. ^{51}Cr as a Neutrino Source. The ^{51}Cr source emits neutrino with energy 0.75 MeV (90.1%) and 0.43 MeV (9.9%). Both of these lines can be detected by gallium–germanium telescope. However, since 96% of captures on Ga is from neutrino with energy 0.75 MeV, the source can be considered with a good approximation as monochromatic one.

^{51}Cr will be produced by neutron capture on ^{50}Cr in SM reactor of the Research Institute of Atomic Reactors (Dimitrovgrad, Ulyanovsk region). Its main feature is the high flux of the thermal neutrons: up to $5.0 \cdot 10^{15}$ cm$^{-2} \cdot$ s^{-1} in the central channel, the average value is $5.0 \cdot 10^{14}$ cm$^{-2} \cdot$ s^{-1}. The central neutron trap of the reactor has 27 channels with a diameter of about 12 mm, so the dimension of the target must be restricted because of limited volume of the central neutron trap. The best irradiation conditions are realized using metal ^{50}Cr with high enrichment up to 97%. According to the calculations, the total source activity will be 3.20 MCi after irradiation of 3015 g of the enriched metallic ^{50}Cr for 59 effective days.

1.2. Metallic Chromium Manufacturing. The natural chromium consists of four stable isotopes ^{50}Cr, ^{52}Cr, ^{53}Cr, ^{54}Cr. The isotope of interest, ^{50}Cr, represents only 4.35% of natural chromium. Therefore, the first step in source production will be the ^{50}Cr enrichment. We propose to use the gas centrifugation of chromyl fluoride CrO_2F_2 due to its rather high efficiency and low cost. Chromyl fluoride is an appropriate volatile compound due to its chemical and physical properties: 1) rather high saturation vapor pressure at room temperature ($>$ 5–10 mm Hg); 2) inactivity to equipment materials; 3) existence of the only one stable isotope of oxygen and fluorine; 4) thermal and chemical stability (no transition in nonvolatile substances). It is necessary to note that the production of chromium CrO_2F_2 is a special non-industrial technology. The chromium enrichment of not less than 97% will be carried out at the JSC PA "Electrochemical Plant" (Zelenogorsk, Krasnoyarsk krai).

After centrifugation, the chromyl fluoride will be transformed into the chromium trioxide CrO_3 by the hydrolysis according to reaction: $CrO_2F_2 + H_2O \rightarrow CrO_3 + 2HF$. Then CrO_3 will be converted into metallic chromium by the electrolysis technique, i.e., in water solution of sulphuric acid using the pure electrolytic copper as a cathode and the lead as an anode.

1.3. Chromium Powder Compaction by Hot Isostatic Pressing. The next technological stage is hot isostatic pressing (HIP) of chromium powder. This rather unique present-day technique is used particularly to convert powder in the solid state, resulting in better physical properties than those achieved by traditional melting or press technologies.

Hot isostatic pressing is a form of heat treatment under high pressure in an inert gas medium. The simultaneous application of heat and pressure eliminates internal voids and microporosity through a combination of plastic deformation, creep, and diffusion bonding. The pilot HIP experiments were performed at the JSC "Kompozit" and first results are presented below.

HIP process consists of several stages (Fig. 2):

1. The production of the metallic powder with the required particle size. Usually a powder is produced by inert gas atomization. We propose to mill the chromium chips until the powder particle size is 56–280 μm. In the first experiments, we used commercially available powder from high-purity refined electrolytic chromium containing the base element 99.98% Cr.

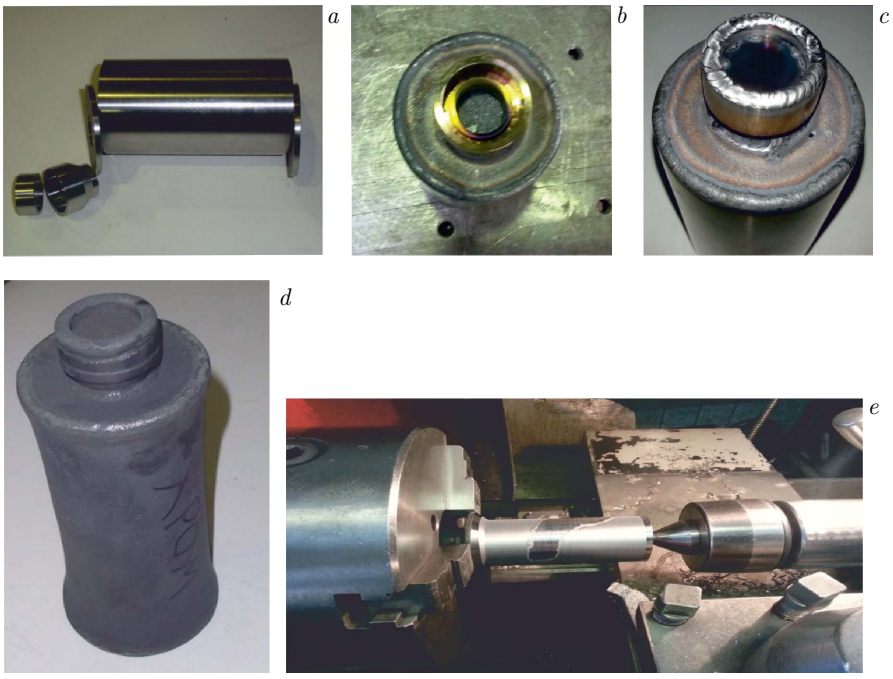

Fig. 2. Main of the HIP technological stages and the finished chromium bars: *a*) capsule details; *b*) capsule filled with powder; *c*) sealed capsule; *d*) capsule after HIP; *e*) mechanical operation of bars

Fig. 3. Finished chromium bars after HIP

2. The calculation and production of the capsule. The capsule must ensure 100% density of chromium bar and the required dimensions.

3. Filling the capsule with metallic powder.

4. Evacuating (up to 10^{-4} Torr) and sealing the capsule.

5. Placing the capsule in a hot isostatic press where it is subjected to high pressure and temperatures (1220°C) during 3 h.

6. Mechanical treatment of bars.

In Fig. 3, the final chromium bars are presented.

1.4. Electrical Discharge Machining of Chromium Bars. The next technological stage is the cutting of chromium rods. We propose to use the rather new technique called Electrical Discharge Machining (EDM) that ensures the removal of very tiny pieces of metal from the workpiece by means of electric spark erosion at a controlled rate by passing high-frequency current through the electrode to the workpiece. In the wire-cut EDM a thin continuous-traveling vertical metal wire (usually brass) in conjunction with deionized water allows the wire to cut through metal by the use of heat from electric sparks. The cut pattern is demonstrated in Fig. 4. The pilot EDM cutting of chromium bars was provided in the Moscow State University of Technology "STANKIN" using SEIBU M500SG equipment.

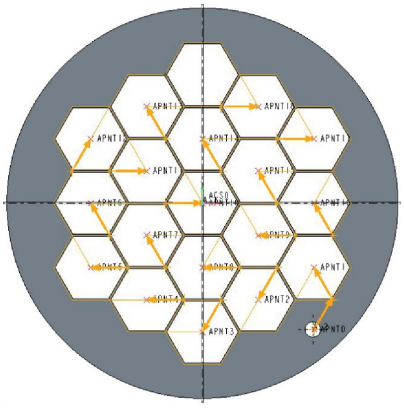

Fig. 4. The cut pattern for wire moving in the EDM of Cr bars

The EDM technique is most attractive for us because of its low-waste technology that allows getting the hexagonal rods without high losses of chromium [10]. Figure 5 shows the hexagonal chromium rods together with titanium separator that will be disposed in the neutrino source.

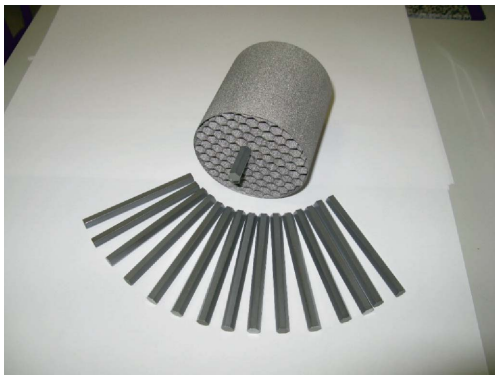

Fig. 5. Chromium rods and titanium separator

The chromium yield amounted to 95% after EDM. We plan to utilize the remains in the next HIP and EDM processes in order to use enriched chromium as effectively as possible.

2. METALLIC CHROMIUM PROPERTIES

2.1. The Metallographic Analysis and Density Measurements. The metallographic analysis of two chromium bars after HIP and EDM processes was carried out at the Research Material Property Laboratory of the University "STANKIN". The metallographic samples were cut from the central and peripheral parts of each bar and then they were polished and etched in 20% water solution of H_2SO_4 at 70°C during 30 min. The metallographic analysis was carried out using optical microscope Carl Zeiss AxioObserver.D1m.

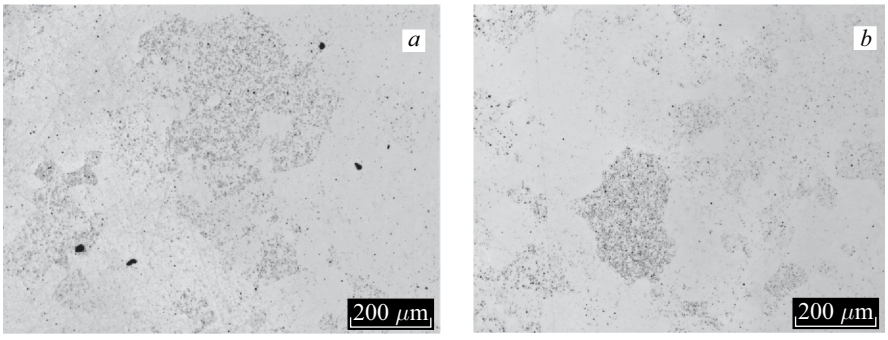

Fig. 6. Porosity of the samples cut from central (*a*) and peripheral (*b*) parts of chromium bars

Table 1. **The data of porosity of two chromium bars**

Sample	Porosity, %	Pore average size, μm
1st bar, center	0.24	1.94
1st bar, periphery	0.16	2.58
2nd bar, center	0.13	1.90
2nd bar, periphery	0.21	2.56

Figures 6, *a* and *b* and Table 1 demonstrate the porosity of the samples cut from central (*a*) and peripheral (*b*) parts of chromium bars. The small pores (3–8 μm) are observed in all sample parts, whereas the big pores (20–30 μm) appear in the peripheral region only.

The average chromium density is (7.19 $\pm$ 0.04) g/cm^3. This value corresponds to tabular data 7.19 g/cm^3 [11]. The density and porosity data show good physical quality of the obtained material.

2.2. Radionuclide Impurity. A serious question in the production of neutrino source is the chromium chemical purity. It is important with a view to the radiation protection and determination of source activity by the calorimetric method.

We investigated the chemical composition of Cr bars after EDM by using a scanning electron microscopy and mass spectroscopy with inductivity coupled plasma. The results are presented in Fig. 7 and Table 2.

The significant amounts of copper and zinc on the bar surface can be explained by using the brass wire during the EDM. However, the contamination depth is about 4 μm and chemical etching in the nitric acid can purify this affected layer. Mainly the impurity concentrations are less than the detection limits of method. Again, Cu and Zn are the main contamination impurities, but the contents of these elements are rather low, about 10 ppm. Table 3 displays the

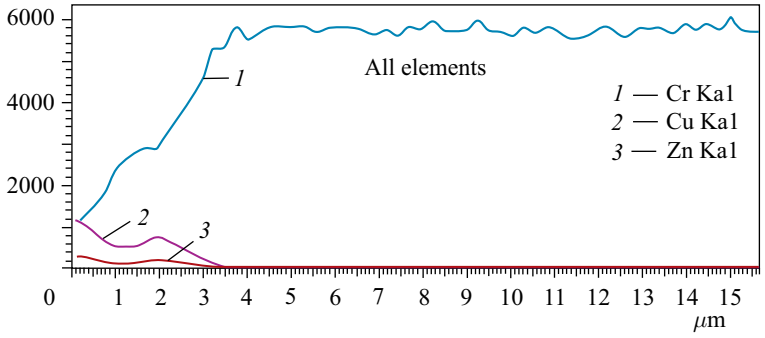

Fig. 7. Distribution of the main elements in surface layer of the chromium bar

Table 2. **Impurity concentrations of the bulk chromium bar**

Element	Concentration, ppm	Element	Concentration, ppm	Element	Concentration, ppm	Element	Concentration, ppm
Li	< 0.1	Zn	10	Sb	< 0.5	Yb	< 0.02
Be	< 0.04	Ga	< 1	Te	< 0.1	Lu	< 0.01
B	< 4	Se	< 3	Ba	< 0.2	Hf	0.1
Na	< 12	Rb	< 1	La	< 0.2	Ta	< 0.03
Mg	4	Sr	< 0.4	Ce	< 0.2	W	0.4
Al	< 1	Y	< 0.1	Pr	< 0.03	Re	< 0.03
Ca	< 11	Zr	< 0.4	Nd	< 0.1	Ir	< 0.01
Sc	< 0.4	Nb	0.62	Sm	< 0.1	Pt	< 0.00
Ti	< 14	Mo	0.79	Eu	< 0.2	Au	< 0.11
Cr	Basis	Rh	< 0.2	Gd	< 0.2	Hg	< 0.5
Mn	< 2	Pd	$< 0,3$	Tb	$< 0,02$	Tl	$< 0,03$
Fe	< 12	Ag	< 0.06	Dy	< 0.07	Pb	< 0.8
Co	< 0.1	Cd	< 0.03	Ho	< 0.02	Bi	< 0.01
Ni	< 1	In	< 0.04	Er	< 0.04	Th	< 0.01
Cu	10	Sn	< 2	Tm	< 0.03	U	< 0.003

Table 3. **Measured impurity in the previous Ga rods prior to activation and the predicted and measured activities. Column 3 displays the present bar data**

Element	Concentration, ppm	Concentration, ppm (present)	Nuclide	Half-life	Activity, mCi	
					Expected	Measured
Fe	50.0	< 12	^{59}Fe	44.5 d	9	24 ± 3
W	25.0	< 0.3	^{187}W	23.9 h	23	Negligible
Cu	15.0	< 10	^{64}Cu	12.7 h	< 0.1	Negligible
Ca	5.7	< 11	^{72}Ga	14.1 h	< 0.1	Negligible
Na	3.3	< 12	^{24}Na	15.0 h	< 0.1	Negligible
Zn	3.3	10	^{65}Zn	244 d	17	Negligible
Ta	3.0	< 0.03	^{182}Ta	115 d	1930	38 ± 5
Co	1.0	< 0.1	^{60}Co	5.3 y	81	65 ± 15
Sc	0.9	< 0.4	^{46}Sc	83.3 d	860	1400 ± 15
As	0.6		^{76}As	26.3 h	2	Negligible
Sb	< 0.1	< 0.5	^{124}Sb	60.2 d	< 13	Negligible
La	< 0.1	< 0.2	^{140}La	40.3 h	< 0.4	Negligible

impurity concentrations of the Cr rods with predicted and measured activities at the beginning of the irradiation in the previous SAGE source experiment.

The analysis of ^{50}Cr in the performed ^{51}Cr experiment showed that the detected impurity concentrations were considerably less than the allowed levels [12]. The third column in Table 3 shows the same impurity concentrations of the present

Cr rods after EDM process. In general, concentrations of the dangerous impurities in the present Gr rods are considerably less than in previous Gr experiment. Therefore, we hope to get a more "pure" neutrino source.

CONCLUSIONS

The technology of production of metal chromium target from ^{50}Cr enriched chromyl fluoride has been developed. The main technological stages are the hydrolysis of chromyl fluoride, the electrochemical reduction of metallic chromium, the hot isostatic pressing of chromium powder and the electrical discharge machining of chromium bars. Pilot hot isostatic pressing and electrical discharge machining of Cr rods experiments showed that the developed techniques ensure the needed physical properties and radionuclide purity of the metallic chromium. With use of the EDM technique, the chromium yield amounted to 95%.

Experimental verification of production and hydrolysis of chromyl fluoride, of electrolysis of CrO_3, of manufacture of metallic Cr powder and the study of purity of chromium and of chromium yield after completing these stages is the next phase of our work.

Acknowledgements. This work has been supported in part by the Russian Foundation for Basic Research under grant No. 13-02-12075 and in part by the Ministry of Education and Science of the Russian Federation in the framework of governmental task in the field of scientific activities under grant No. 9.1557.2014/K.

REFERENCES

1. *Abdurashitov J. N. et al. (SAGE Collab.)*. Measurement of the Response of a Gallium Metal Solar Neutrino Experiment to Neutrinos from a ^{51}Cr Source // Phys. Rev. C. 1999. V. 59. P. 2246–2263.
2. *Kaether F. et al.* Reanalysis of the Gallex Solar Neutrino Flux and Source Experiments // Phys. Lett. B. 2010. V. 685. P. 47–54.
3. *Bahcall J. N.* Gallium Solar Neutrino Experiments: Absorption Cross Sections, Neutrino Spectra, and Predicted Event Rates // Phys. Rev. C. 1997. V. 56. P. 3391–3409.
4. *Frekers D. et al.* The ^{71}Ga(^{3}He, t) Reaction and the Low-Energy Neutrino Response // Phys. Lett. B. 2011. V. 706. P. 134–138.
5. *Abazajian K. N. et al.* Light Sterile Neutrinos: A White Paper. arXiv:1204.5379v1 [hep-ph]. 2012.
6. *Aguilar A. et al. (LSND Collab.)*. Evidence for Neutrino Oscillations from the Observation of Antineutrino (Electron) Appearance in an Antineutrino (Muon) Beam // Phys. Rev. D. 2002. V. 64. P. 112007.

7. *Aguilar-Arevalo A. A. et al. (MiniBooNE Collab.).* Search for Electron Antineutrino Appearance at the $\Delta m^2 \sim 1$ eV^2 Scale // Phys. Rev. Lett. 2009. V. 103. P. 111801.
8. *Mueller T. A. et al.* Improved Predictions of Reactor Antineutrino Spectra // Phys. Rev. C. 2011. V. 83. P. 054615.
9. *Gavrin V. et al.* Current Status of New SAGE Project with ^{51}Cr Neutrino Source // Phys. Part. Nucl. 2015. V. 46, No. 2. P. 131–137.
10. *Molodtsov V. V., Okunkova A. A., Peretyagin P. Yu.* Manufacture of Graphite Electrodes for the Electrospark Machining of Complex High Precision Components // Rus. Engin. Res. 2012. V. 32, No. 7–8. P. 550–552; DOI: 10.3103/S1068798X12060160.
11. *Babichev A. P., Babuschkina N. A., Bratkovsky A. M.* Physical Quantities. M:. Energoatomizdat, 1991. 1232 p. (in Russian).
12. *Cribier M. (GALLEX Collab.)* // Production of a 62 PBq ^{51}Cr Low Energy Neutrino Source for GALLEX // Nucl. Instr. Meth. A. 1996. V. 378, No. 1–2. P. 233-250.